Journal of Photochemistry and Photobiology A: Chemistry 202 (2009) 81–85

Contents lists available at ScienceDirect

Journal of Photochemistry and Photobiology A: Chemistry

journal homepage: www.elsevier.com/locate/jphotochem

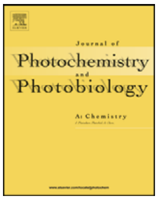

One pot direct hydrothermal growth of photoactive TiO_2 films on glass

Dimitra Vernardou[a,b,c], Emmanouil Stratakis[c,d,e], George Kenanakis[a,b,f], Heather M. Yates[g], Stelios Couris[h,i], Martyn E. Pemble[j,*], Emmanouil Koudoumas[a,d], Nikos Katsarakis[a,b,e]

[a] Centre of Materials Technology and Laser, School of Applied Technology, Technological Educational Institute of Crete, 710 04 Heraklion, Crete, Greece
[b] Science Department, School of Applied Technology, Technological Educational Institute of Crete, 710 04 Heraklion, Crete, Greece
[c] University of Crete, Department of Materials Science and Technology, 710 03 Heraklion, Crete, Greece
[d] Electrical Engineering Department, Technological Educational Institute of Crete, 710 04 Heraklion, Crete, Greece
[e] Institute of Electronic Structure and Laser, Foundation for Research & Technology-Hellas, P.O. Box 1527, Vassilika Vouton, 711 10 Heraklion, Crete, Greece
[f] University of Crete, Department of Chemistry, 710 03 Heraklion, Crete, Greece
[g] Institute for Materials Research, University of Salford, Cockroft Building, Salford, Manchester M5 4WT, UK
[h] Institute of Chemical Engineering and High Temperature Chemical Processes (ICE-HT), Foundation for Research and Technology-Hellas (FORTH), 26504 Patras, Greece
[i] University of Patras, Department of Physics, 26504 Patras, Greece
[j] Tyndall National Institute, University College Cork, Lee Maltings, Prospect Row, Cork, Ireland

ARTICLE INFO

Article history:
Received 22 August 2008
Received in revised form 31 October 2008
Accepted 4 November 2008
Available online 7 December 2008

Keywords:
Hydrothermal growth
Titania
Photoactivity
Anatase
Thin films

ABSTRACT

We demonstrate that titanium (IV) oxide films may be deposited on Corning glass by a simple, one-pot, low temperature (95 °C) hydrothermal growth technique and that providing the correct conditions are employed, the films produced show clear photoactivity under UV illumination as evidenced by changes in water contact angle and the progressive photo-oxidation of stearic acid. It is further demonstrated that the growth, structure and photoactivity of the films depends critically upon the H_2O concentration employed during growth. For H_2O concentrations below 0.1 M, little or no growth was observed, while above 0.3 M, precipitation or even gelation rapidly occurred. Only at H_2O concentrations of 0.1 M and 0.2 M was appreciable film growth observed, while photoactive titania was formed only via growth using a water concentration of 0.1 M, the films grown using the higher concentration of water (0.2 M) being essentially photo-inactive. The method developed is discussed in terms of the possible chemical steps involved and is proposed as a low-cost alternative to higher temperature, less environmentally friendly approaches to TiO_2 film production.

1. Introduction

Titanium (IV) oxide (TiO_2), particularly in the anatase form, finds extensive application in a wide range of technologies including optical cells [1], solar energy conversion [2], photocatalysis [3], anti-fogging and self-cleaning or anti-bacterial coatings [4]. These light-induced properties arise because TiO_2 has a wide direct electron energy band gap equivalent to radiation in the UV part of the spectrum, transparency throughout the visible spectrum and a high refractive index over a broad spectral range from the ultraviolet to the far infrared [5]. There are three types of TiO_2 crystalline structure: anatase, rutile and brookite [6]. Anatase and rutile are found to be the most suitable for photo-induced applications of TiO_2, and amorphous material displays little or no photoactivity. Although rutile is a more thermodynamically stable structure and exhibits higher refractive index (2.61–2.90) [7], the most commonly used form of TiO_2 for photo-induced applications is anatase [8].

The synthesis of TiO_2 films with specific, tailored properties is of great importance in terms of the technology applications noted above. Films consisting of particles with dimensions smaller than several tens of nanometers (nanoparticles) are of great interest because they often exhibit improved mechanical, optical and chemical properties compared with the bulk material [9]. For the deposition of TiO_2 films, nanoparticles or films consisting of aggregates of nanoparticles, several techniques have been employed including chemical vapour deposition (CVD) [10], hydrolysis [11], sol–gel methods [12], micro-emulsion (or reverse micelle systems) [13], and hydrothermal synthesis [14–16], most of them requiring quite high temperatures and toxic chemicals. Of these, hydrothermal growth seems to be a more environmentally friendly and low cost technique, since low temperatures are employed and, in general, no toxic chemicals are required. In such a case, the precursor solutions, the growth temperature and the deposition time can have a significant effect on the morphological and structural properties of the final products [17].

---

[*] Corresponding author. Tel.: +353 214904456; fax: +353 214270271.
E-mail address: martyn.pemble@tyndall.ie (M.E. Pemble).

1010-6030/$ – see front matter © 2008 Elsevier B.V. All rights reserved.
doi:10.1016/j.jphotochem.2008.11.015

In this work, we have studied the growth of TiO_2 thin films on Corning glass using a simple, one pot hydrothermal synthesis involving water and isopropanol. We find that in contrast to other approaches that have been reported, under appropriate conditions it is possible to grow reversibly photoactive coherent films from aqueous solutions of simple reagents, at temperatures as low as 95 °C.

2. Experimental

In a typical procedure for the solution preparation, 12 M of i-PrOH ($CH_3CH(OH)CH_3$) was first stirred with various amounts of MilliQ H_2O in the range of 0.05 up to 0.5 M, for approximately 10 min. Then, 0.03 M of TTIP ($Ti[(OCH(CH_3)_2)]_4$) was added under continuous stirring for another 5 min. Finally, the solution was placed in a Pyrex glass bottle with polypropylene autoclavable screw cap, with the substrate positioned on the bottom, and was heated at a constant temperature of 95 °C for a specified time in a regular laboratory oven. After this, the samples were thoroughly washed with i-PrOH in order to eliminate residual salts, and dried in air at 95 °C. Prior to deposition, all substrates were ultrasonically cleaned with i-PrOH, acetone, MilliQ H_2O and dried with N_2. Finally, for a better insight in the structure of the films, all samples were annealed at 500 °C for 2 h under ambient conditions.

X-ray diffraction (XRD) measurements were performed using a Rigaku (RINT 2000) Diffractometer with Cu Kα X-rays, while, Raman measurements were carried out using a model Raman Spectrometer (Jobin Yvon, ISA – Horiba group model T-64000), using a 514.5 nm line of an air-cooled Ar^+ laser (Spectra-Physics 163-A42) and wavenumber range 50–750 cm^{-1}. X-ray photoelectron spectroscopy (XPS) (Kratos AXIS Ultra), performed using an Al (monochromated) Kα radiation source, was used to analyze the surface composition and stoichiometry of the films. During the measurements, it was necessary to use a charge neutraliser since the samples were insulating, due mainly to the deposition on glass. This tends to shift the peak positions by up to 2 eV and for this reason the measurements are referenced to the residual C 1s signal at 285 eV. Curve fitting was performed using CASA XP software with a mixture of Gaussian–Lorentzian functions to deconvolute spectra. UV–vis measurements were performed using a PerkinElmer Lambda 950 spectrometer over the wavelength range of 200–1000 nm. Surface imaging was carried out on an atomic force microscope (AFM) in tapping mode (Digital Instruments – Nanoscope IIIa). Silicon cantilevers (TESP Si probes-Veeco) were used to obtain topographic information about the film surface. Contact angle measurements were performed by the sessile drop method. A 10 μl distilled, deionised Millipore H_2O droplet was gently positioned on the surface using a microsyringe. A CCD camera-lens optical system was used to capture digital images of the droplet profile from a location parallel to the substrate. Contact angles were subsequently determined from the corresponding pictures using an image-processing algorithm. The mean value was calculated from at least five individual measurements. Light induced hydrophilicity was evaluated by irradiating the samples at certain time intervals with 4 mW cm^{-2} UV light of a Hg lamp, centred at 365 nm, in atmospheric air and a temperature of 25 °C. After each time interval, a 10 μl H_2O droplet was placed on the irradiated area and the corresponding contact angle was measured again. Following irradiation, the samples were stored in the dark at room temperature for 7 days and then the respective contact angles were measured again. Each characterization method was completed on at least three samples prepared under the same conditions for consistency and reproducibility.

Stearic acid testing was performed after spin coating the samples using a 30 μl droplet of stearic acid in chloroform (0.1 M solution) spun at a rotation speed of 2000 rpm for 30 s. Samples were then thoroughly dried at 80 °C in air for 10 min. The IR absorbance of the C–H stretching region of the stearic acid spectrum (2800–3000 cm^{-1}) was then recorded using a FTIR spectrometer (IRPRESTIGE-21, Shimadzu), in transmission mode before and after illumination with a UV lamp centred at 365 nm (black light blue lamps). The lamp power density at the sample was 2 mW cm^{-2} and the samples were exposed to the lamp for various times before the IR data was recorded.

3. Results and discussion

A standard growth time of 20 h was selected for these studies based on consideration of a range of similar procedures reported in the literature [18,19] and after observing that growth times of less than 15 h resulted in films which displayed no photoactivity, no matter what initial solution was used. Under these conditions we have found that the nature of the growth depends critically upon the concentration of water in the initial solution. If this quantity was below 0.1 M, we observed very little if any growth. When it was around 0.2 M, growth became patchy and uneven, while increasing the water concentration still further to ca. 0.3 M, we observed gelation and no coherent hydrothermal growth occurred. The concentration of water clearly influences the solution chemistry and by implication, also the growth chemistry that occurs at the substrate surface. In our study, we have observed that it was only possible to generate coherent films suitable for subsequent analysis if water concentrations in the range 0.1–0.2 M were employed in the initial solution. The deposited films were found to have a very good adhesion passing the Scotch tape test and were stable in air for over 6 months. All samples presented an almost flat transparency, exhibiting about 70–80% transmission in the range from 380 nm up to NIR.

Analysis of these films has shown that the procedure described only produces photoactive titania under conditions where the initial water concentration in the solution was 0.1 M. Fig. 1 reveals this by presenting data for the variation in water contact angle with increasing time of exposure of the films to UV radiation. The H_2O contact angle of all deposited films was measured to be in the range of 75–80° before any light illumination, indicating hydrophobicity. For samples grown with initial water concentrations of 0.2 M and 0.3 M, it may clearly be seen that the contact angle does not vary appreciably under UV illumination. However, for the sample prepared using an initial water concentration of 0.1 M, clear evidence of the progressive decrease in water contact angle is seen, with increasing exposure to UV radiation. Interestingly, Fig. 1 also shows that the rate of change of contact angle with exposure time

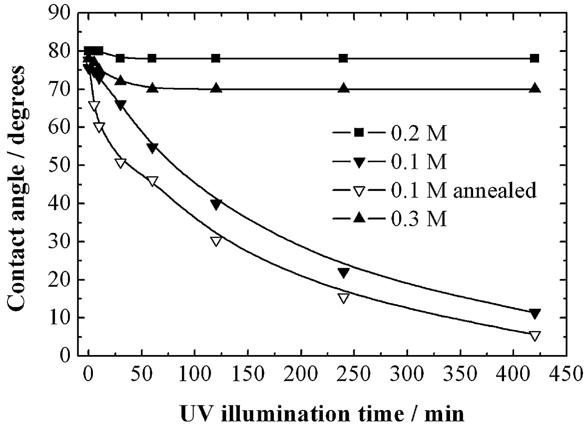

Fig. 1. H_2O contact angle dependence on UV illumination time of TiO_2 thin films for 0.1 M (as-deposited and annealed), 0.2 M and 0.3 M using 4 mW cm^{-2} UV light of a Hg lamp, in atmospheric air and temperature of 25 °C.

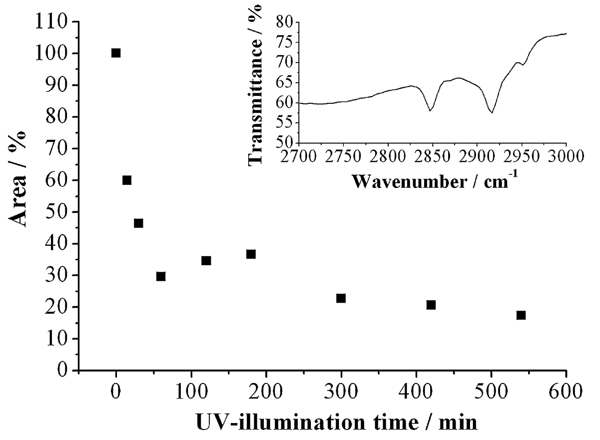

Fig. 2. Area under the C–H stretching of the stearic acid spectrum (inset) dependence on UV illumination time of TiO_2 thin films for 0.1 M (as-deposited), using 2 mW cm^{-2} UV light centred at 365 nm, in atmospheric air and temperature of 25 °C.

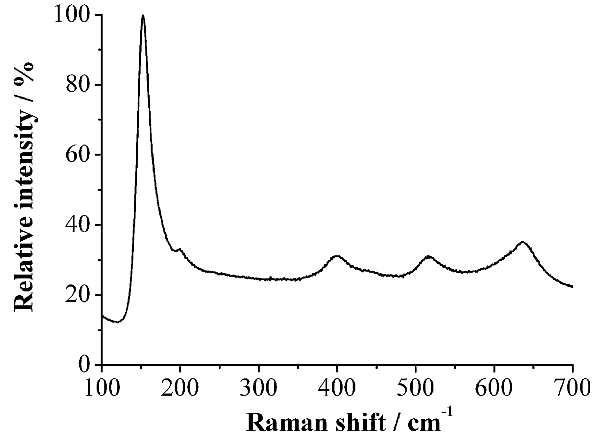

Fig. 4. Raman spectrum of as-deposited TiO_2 films on Corning glass by hydrothermal growth using 0.1 M MilliQ H_2O at 95 °C for deposition time of 20 h.

increases quite dramatically after the films that demonstrate photoactivity were annealed at 500 °C for 2 h.

For the active samples, i.e. those grown using an initial water concentration of 0.1 M, the H_2O droplet spread out on the film surface after approximately 250 min of irradiation under UV light, to yield a contact angle of about 12°, which indicates superhydrophilicity. Furthermore, the contact angle was observed to return to its initial value after storing the samples in dark at room temperature.

For the photoactive as-grown films (0.1 M MilliQ H_2O concentration), further evidence of their photoactivity comes from conventional UV-induced stearic acid degradation tests (Fig. 2). It demonstrates clearly that on the same time scales as those which give rise to the drop in contact angle, the stearic acid film was appreciable degraded.

Given that the conditions under which photoactive films were produced, were found to be critically dependent on the initial water concentration in the solution, it was appropriate to consider whether the different growth conditions produced different materials in terms of crystallinity and morphology. The basic premise here being that the most photoactive films would be the most crystalline and also perhaps the roughest—with the highest specific surface area, although it is always very hard to effectively correlate observed photoactivity measurements with surface area or surface roughness data.

In terms of film crystallinity, Fig. 3 shows a representative XRD pattern for the as-deposited material (a) and the annealed material (b) on Corning glass. The TiO_2 films used for these experiments were prepared using a solution containing 0.1 M MilliQ H_2O at 95 °C for a deposition time of 20 h, i.e. using the same conditions that were found to give rise to photoactive films. The data for the as-deposited material shows no evidence of any diffraction peaks, indicating that the deposited film was largely amorphous. The broad feature observed from 20° to 37° is due to the underlying substrate. Thus on the basis of XRD alone we might conclude that the films are not crystalline anatase and that furthermore, as a consequence, they would not be photoactive. However, the data shown in Figs. 1 and 2 demonstrate that this latter statement is clearly incorrect.

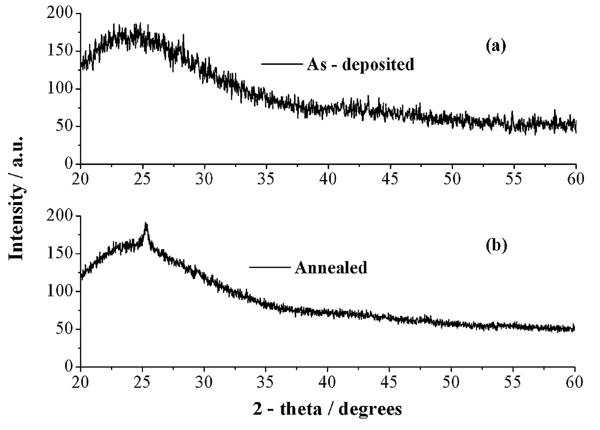

Fig. 3. XRD analysis of as-deposited (a) and annealed (b) TiO_2 films hydrothermally grown on Corning glass using 0.1 M MilliQ H_2O at 95 °C for deposition time of 20 h.

Annealing the as-grown samples resulted in the appearance of one characteristic peak at a 2θ value of 25.3° (Fig. 3(b)), which would be consistent with an assignment to the diffraction from the [1 0 1] planes of anatase [20]. Thus it would appear that using XRD, only the annealed films show any kind of evidence of anatase formation, despite the fact that both as-grown and annealed films exhibit photoactivity. Since this was a somewhat surprising result, the films were also studied using Raman spectroscopy (Fig. 4).

Fig. 4 shows the Raman spectrum of the as-deposited film grown on Corning glass for 0.1 M of H_2O concentration and a deposition time of 20 h. It is of great significance that films grown under these conditions were the only films to exhibit any kind of phonon structure in the Raman spectra obtained. The observed phonon frequencies, matching (± 2 cm^{-1}) with literature [21] for anatase TiO_2 are: 147 cm^{-1} (E_g), 200 cm^{-1} (E_g), 400 cm^{-1} (B_{1g}), 517 cm^{-1} (A_{1g}) and 640 cm^{-1} (E_g).

Thus, although XRD evidence alone does not definitively identify the formation of anatase in either the as-grown or annealed films, Raman analysis does point to the formation of anatase. This observation, coupled with the photoactivity of the films observed, leads us to conclude that our recipe for the hydrothermal growth of TiO_2 on glass does result in the formation of a film that contains some crystalline anatase but exactly how much it is difficult to assess at this stage. Perhaps most noteworthy is the fact that the concentration of the water in the initial solution appears to be a critical factor, in that if this figure is above 0.1 M, then no photoactivity is seen while the Raman and XRD data also show no evidence of any crystallisation of the material.

The surface composition of the as-deposited films grown using the conditions needed to generate photoactive material, has been examined using XPS (Fig. 5(a) and (b)). A broad scan was used as a qualitative measure of the elements present on the sample, and high resolution scans of the characteristic regions of the respective elements were used for the quantitative analysis and peak fitting. All analysis of the samples showed that elements present on the

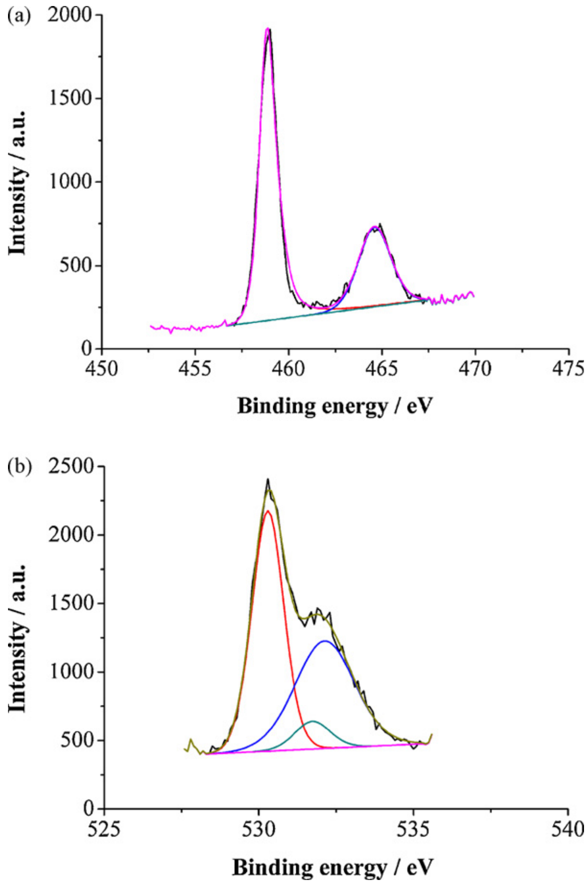

Fig. 5. XPS deconvoluted spectra of Ti 2p (a) and O 1s (b) peaks of a TiO_2 film deposited on Corning glass using 0.1 M MilliQ H_2O for deposition time of 20 h by hydrothermal growth. The black line is the raw data, while the other lines represent the deconvoluted fits for both figures.

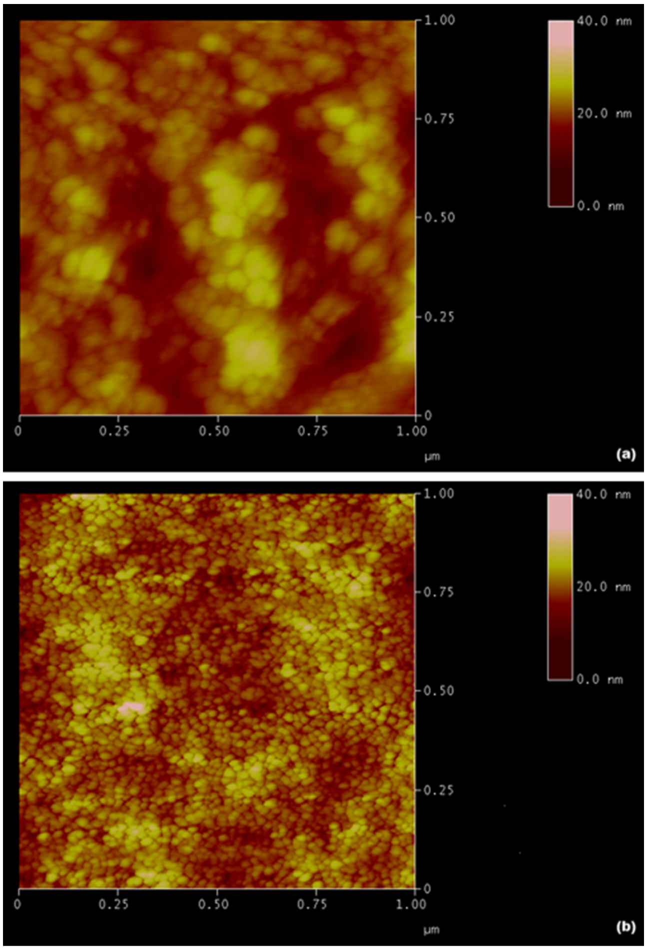

Fig. 6. AFM images of TiO_2 films deposited on Corning glass using hydrothermal growth for 0.1 M MilliQ H_2O, as-deposited (a) and annealed (b).

surface were Ti, O and C, along with very small amounts of Si and N. The N signal at 400 eV related to traces of molecular chemisorbed N_2 [22]. The Si signal was assigned to SiO_2 [23], which was confirmed by the presence of a deconvoluted peak at 532.1 eV in the high resolution O 1s spectrum (Fig. 5(b)). Considering the nature of the sample, the peaks associated with SiO_2 are due to the glass substrate. The high resolution scan for the Ti 2p (Fig. 5(a)), yields a $2p_{3/2}$ peak at 458.9 eV and a splitting of 5.8 eV, which relates to Ti^{4+} bound to O^{2-} [24]. In turn the O 1s signal could be resolved into 3 peaks, as seen in Fig. 5(b). The most intense peak at 530.3 eV assigned to O^{2-} bound to Ti^{4+}, which confirmed the presence of TiO_2. The remaining peaks related to SiO_2, as previously mentioned and O in absorbed water (531.7 eV) [25]. By further fitting of the data and calculation it was possible to establish that the TiO_2 was stoichiometric.

The extent of disorder within a structure can be judged by the broadness of the Ti 2p signal [26]. The width of the Ti 2p peaks (measured from the full width at half maximum peak height) was 0.97 eV ($2p_{3/2}$). Comparison with the splitting measured in XPS spectra from highly ordered TiO_2 films grown by CVD (0.74–0.87 eV) [27] showed that the disorder in the films deposited in this present work is only a fraction higher, and certainly less than that observed previously for other TiO_2 films, for example in the work of Prieto and Kirby who noted a line broadening on the order of 1.62 eV, which they attributed to a disordered sample [26].

Turning now to surface morphology, since this clearly impinges on photocatalytic activity, Fig. 6(a) and (b) present high resolution AFM images of the as-deposited and annealed films grown using the low H_2O concentration conditions. Although these images are not highly informative, what is clear is that the image of the as-deposited film, Fig. 6(a), indicates fully developed, compact nanoparticles, forming fine agglomerations on the substrate, while the annealed film (Fig. 6(b)) shows more closely packed, smaller nanoparticles with uniform size. The average particle sizes were 50 nm and 20 nm for the as-grown and annealed samples respectively. The fact that the average particle size decreases upon annealing is particularly noteworthy as it implies that partial crystallisation of the film results in a major change in morphology. However, once again it is very difficult to gauge just exactly how crystalline the samples become after annealing since although Fig. 1 demonstrates that the photoactivity increases, Fig. 3 reveals that by XRD the changes in crystallinity are very small. In fact, it could be argued that the increase in photoactivity observed arises only from the decrease in particle size and the subsequent increase in specific surface area. Clearly these factors need further examination.

It is appropriate to consider the nature of the processes occurring during hydrothermal growth as employed in our experiments. For this purpose, we present below a series of simple equations, which are not meant to be a complete or exclusive mechanistic description, but rather which demonstrate some possibilities that are consistent with the known chemistry of these systems.

The reaction in question may be expressed as follows:

$$Ti[(OCH(CH_3)_2)]_4 + 2H_2O \leftrightarrow TiO_2 + 4CH_3CH(OH)CH_3 \quad (1)$$

One may imagine that via oxygen lone pair attack of the vacant octahedral sites around the Ti^{4+} centre such that proton and hydroxyl ion transfer may occur so as to retain two Ti–O bonds and cleave two others. According to the reaction (1), the reaction of each TTIP molecule liberates four isopropanol molecules. If it is assumed that under hydrothermal growth conditions this reaction is reversible, then the influence of isopropanol on the reaction is immediately apparent in that it may inhibit the forward reaction and actively promote the reverse reaction. However, it is also quite possible that the reaction proceeds more like a series of sequential steps, with Ti^{4+} hydroxyl species as intermediates, Scheme (2):

$$\mathrm{Ti[(OCH(CH_3)_2)]_4} + n\mathrm{H_2O} \leftrightarrow \mathrm{Ti(OH)}_n\mathrm{[(OCH(CH_3)_2)]}_{4-n} + n\mathrm{CH_3CH(OH)CH_3} \quad (2)$$

where $n = 1–4$.If this were the case, then the conversion of the hydroxide species to TiO_2 would occur via a condensation reaction, eliminating water, Scheme (3):

$$\mathrm{Ti(OH)_4} \leftrightarrow \mathrm{TiO_2} + 2\mathrm{H_2O} \quad (3)$$

If it is assumed that under the isolated conditions employed in hydrothermal growth that all reactions are reversible as shown, the influence of water on the possible dissolution and gelation processes becomes apparent from Schemes (2) and (3). Intermediate hydroxides as well as $Ti(OH)_4$ itself have the opportunity to form the extended network or polymer like structure expected for a gel, while water itself may inhibit TiO_2 formation. Under normal reaction conditions because of the stability of TiO_2 thermodynamic factors are likely to dominate. However under hydrothermal conditions it may be that the reaction proceeds by kinetic control, based on the complex interplay of processes such as those depicted in Schemes (1)–(3).

In reality very little is known regarding the true nature of these processes, other than that they are complex and clearly much work is required in order to try to identify the key mechanistic steps involved. However, the processes presented here appear to be consistent with our findings, as discussed below.

It would seem that during the hydrothermal process, it is amorphous TiO_2 that forms initially and then this is slowly transformed to anatase as a result of the interplay of complex deposition and dissolution processes, all of which create changing concentration gradients of reagents at the growing surface. In the course of our studies it was found that a H_2O concentration greater than 0.3 M resulted in solutions where precipitation and gelation occurred. The implication here is that higher concentration of water promote higher reaction rates, forcing Scheme (1) rapidly to the right, such that the conditions approach those used in TiO_2-based sol–gel formation [28,29]. On the other hand, under conditions of H_2O deficiency (H_2O concentration less than 0.1 M), either no deposition, or only patchy deposition was observed. Again this observation is consistent with Schemes (1)–(3), since H_2O is clearly needed for reaction, yet with an excess of isopropanol already present, the reaction will be biased to the left. In other words, using our arguments presented above we propose that once again the water concentration was strongly influencing reaction rate, in this case reducing the rate at which the TTIP was converted to TiO_2.

The overall chemistry is clearly a trade off between the need for water to initiate the reaction and the influence of reaction products such as isopropanol on reaction rate. Experimentally we have established that a H_2O concentration of ca. 0.1 M appears to be the optimal one, leading to the production of photoactive films that appear to contain at least some anatase as determined by Raman, while also being stoichiometric as determined by XPS.

4. Conclusions

In conclusion, we have demonstrated that under conditions of carefully controlled H_2O concentrations, it is possible to produce photoactive TiO_2 films on glass directly, in a low-temperature, one pot hydrothermal synthesis. We have speculated as to the possible reactions that may be involved in what is quite obviously a complex process and have suggested that kinetic control of growth could account for the observations presented. We propose that our method, although slow, requiring ca. 20 h to develop photoactivity in the films, may find application as a cheap, environmentally friendly method of depositing photoactive titania over a wide range of substrates that may then be used in a range of self-cleaning, anti-bacterial or related applications.

Acknowledgements

MEP gratefully acknowledges the support of Science Foundation Ireland via his Principal Investigator Award number 01/PI.2/C041.

References

[1] B.E. Yoldas, T.W. O' Keeffe, Appl. Opt. 18 (1979) 3133.
[2] M.E. Butler, D.S. Ginley, J. Mater. Sci. 15 (1980) 19.
[3] T. Carlson, G.L. Giffin, J. Phys. Chem. 90 (1986) 5896.
[4] R. Wang, K. Hashimoto, A. Fujishima, Nature 388 (1997) 431.
[5] P. Evans, M.E. Pemble, D.W. Sheel, Chem. Mater. 18 (2006) 5750.
[6] M.P. Moret, R. Zallen, D.P. Vijay, S.B. Desu, Thin Solid Films 366 (2000) 8.
[7] M.L. Hitchman, S.E. Alexandrov, Electrochem. Soc. Interface 10 (2001) 40.
[8] M.Kh. Aminian, N. Taghavinia, A. Iraji-zad, S.M. Mahdavi, M. Chavoshi, S. Ahmadia, Nanotechnology 17 (2006) 520.
[9] L. Tuller, J. Electroceram. 1 (1997) 211.
[10] S.K. Pradhan, P.J. Reucroft, F. Yang, A. Dozier, J. Cryst. Growth 256 (2003) 83.
[11] K.D. Kim, H.T. Kim, Powder Technol. 119 (2001) 164.
[12] T. Sugimoto, K. Okada, H. Itoh, J. Colloid Interface Sci. 193 (1997) 140.
[13] E. Stathatos, P. Lianos, F. DelMonte, D. Levy, D. Tsiourvas, Langmuir 13 (1997) 4295.
[14] M. Wu, G. Lin, D. Chen, G. Wang, D. He, S. Feng, R. Xu, Chem. Mater. 2002 (14) (1974).
[15] S. Yang, L. Gao, J. Am. Ceram. Soc. 88 (2005) 968.
[16] H.Y. Zhu, Y. Lan, X.P. Gao, S.P. Ringer, Z.F. Zheng, D.Y. Song, J.C. Zhao, J. Am. Chem. Soc. 127 (2005) 6730.
[17] K. Byrappa, M. Yoshimura, Handbook of Hydrothermal Technology, William Andrew Publishing, New York, 2001.
[18] M.C. Carotta, S. Gherardi, C. Malagù, M. Nagliati, B. Vendemiati, G. Martinelli, M. Sacerdoti, I.G. Lesci, Thin Solid Films 515 (2007) 8339.
[19] C. Su, C.-M. Tseng, L.-F. Chen, B.-H. You, B.-C. Hsu, S.-S. Chen, Thin Solid Films 498 (2006) 259.
[20] JCPDS-International Centre for Diffraction Data, PDF 21-1272.
[21] Y. Lei, L.D. Zhang, J.C. Fan, Chem. Phys. Lett. 338 (2001) 231.
[22] O. Diwald, T.L. Thompson, E.G. Goralski, S.D. Walck, J.T. Yates, J. Phys. Chem. B 108 (2004) 52.
[23] J. Chastain, R.C. King, Handbook of X-Ray Photoelectron Spectroscopy, Physical Electronic Inc., New York, 1995.
[24] Y.J. Sun, T. Egawa, L.Y. Zhang, X. Yao, Jpn. J. Appl. Phys. 41 (2002) L1389.
[25] X.Y. Li, X. Quan, C. Kutal, Scripta Mater. 50 (2004) 499.
[26] P. Prieto, R.E. Kirby, J. Vac. Sci. Technol. A 13 (1995) 2819.
[27] H.M. Yates, M.G. Nolan, D.W. Sheel, M.E. Pemble, J. Photochem. Photobiol. A 179 (2006) 213.
[28] A. Mills, N. Elliott, G. Hill, D. Fallis, J.R. Durrant, R.L. Willis, Photochem. Photobiol. Sci. 2 (2003) 591.
[29] M. Sasani Ghamsari, A.R. Bahramian, Mater. Lett. 62 (2008) 361.